Yingfei Li
yingfeil@stanford.edu

A computational package for atomic photoemission cross-section

Contents

1 Photo-emission cross-section

1.1 Transition probability and matrix element

The overall photoemission process can be approximately described by a three-step model:

- Excitation of electrons by incident photons;
- Travel of excited photo-electron to the surface;
- Escape of the photo-electron into vacuum.

The first process carries the most important information of electronic structure. This process can be described by the transition probability w_{fi} of an N-electron initial and final state under the framework of Fermi's golden rule:

$$w_{fi} = \frac{2\pi}{\hbar} |\langle \Psi_f^N | H_{\text{int.}} | \Psi_i^N \rangle|^2 \delta(E_f^N - E_i^N - h\nu)$$

, where $|\Psi_f^N\rangle$ is the N-electron initial state and $|\Psi_i^N\rangle$ is the N-electron final state. $H_{\text{int.}}$ is the Hamiltonian describing the interaction between electron and photons. Under dipole approximation and in a non-interacting system, the transition probability becomes

$$w_{fi} \propto |M_{f,i}^{\boldsymbol{k}}|^2 \delta(\epsilon_f - \epsilon_k - h\nu)$$

, where

$$M_{f,i}^{\boldsymbol{k}} = \langle \Phi_{\text{E}_{\text{kin}},\boldsymbol{k}} | \, \hat{\boldsymbol{\epsilon}} \cdot \boldsymbol{r} \, | \Phi_{nlx} \rangle \tag{1.1.1}$$

with $\Phi_{\text{E}_{\text{kin}},\boldsymbol{k}}$ the one-electron final state with kinetic energy E_{kin} and Φ_{nlx} the one-electron initial state in atomic level characterized by quantum number n, l, x elaborated below. $\hat{\boldsymbol{\epsilon}} \cdot \boldsymbol{r}$ is the photon-electron interaction under dipole approximation, with $\hat{\boldsymbol{\epsilon}}$ is the unit electric field vector of incident photon, and $\boldsymbol{r}$ is the position vector.

1.2 Photo-emission cross-section with fixed-orientation

The photo-emission cross-section with fixed-orientation is generally expressed as

$$\frac{d\sigma}{d\Omega}(E_{\text{kin}}) = (\frac{4\pi\alpha_0 a_0^2}{3})(h\nu) |\langle \Phi_{E_{\text{kin}},\boldsymbol{k}} | \, \hat{\boldsymbol{\epsilon}} \cdot \boldsymbol{r} \, | \Phi_{nlx} \rangle|^2 \tag{1.2.1}$$

, where α_0 is the fine-structure constant ($\approx 1/13704$), a_0 is the Bohr radius ($= 0.52918\mathring{A}$), $h\nu$ is the photon energy (in units of Rydberg unit). We address the matrix element term $\langle \Phi_{E_{\text{kin}},\boldsymbol{k}} | \, \hat{\boldsymbol{\epsilon}} \cdot \boldsymbol{r} \, | \Phi_{nlx} \rangle$ in details in section 2 and 3.

1.3 Photo-emission cross-section for total sub-shell

The total nl sub-shell photoemission cross-section for an ensemble of random oriented atoms can be written in the form

$$\sigma(E_{\text{kin}}) = (\frac{4\pi\alpha_0 a_0^2}{3}) \cdot \frac{N_{nl}}{2l+1} \cdot (h\nu) \cdot [lR_{l-1}^2(E_{\text{kin}}) + (l+1)R_{l+1}^2(E_{\text{kin}})] \tag{1.3.1}$$

, where N_{nl} is the number of electrons in the nl sub-shell (i.e. $N_{nl} = 2(2l+1)$ if filled). $R_{l\pm1}(E_{\text{kin}})$ are the integrals of radial wave function define explicitly in eq. 2.1.12.

Eq. 1.3.1 gives the cross-section that are an integrated total over the complete 4π solid angle of acceptance. Differential cross-sections as a functional of α, the angle between the photon propagation direction and electron emission direction, can be obtained for a randomly-oriented ensemble of atoms in an unpolarized radiation field from

$$\frac{d\sigma_{nl}}{d\Omega} = \frac{\sigma_{nl}(E_{\text{kin}})}{4\pi}[1 - \frac{1}{2}\beta_{nl}(E_{\text{kin}}))P_2(\cos\alpha)] \tag{1.3.2}$$

Yingfei Li
yingfeil@stanford.edu

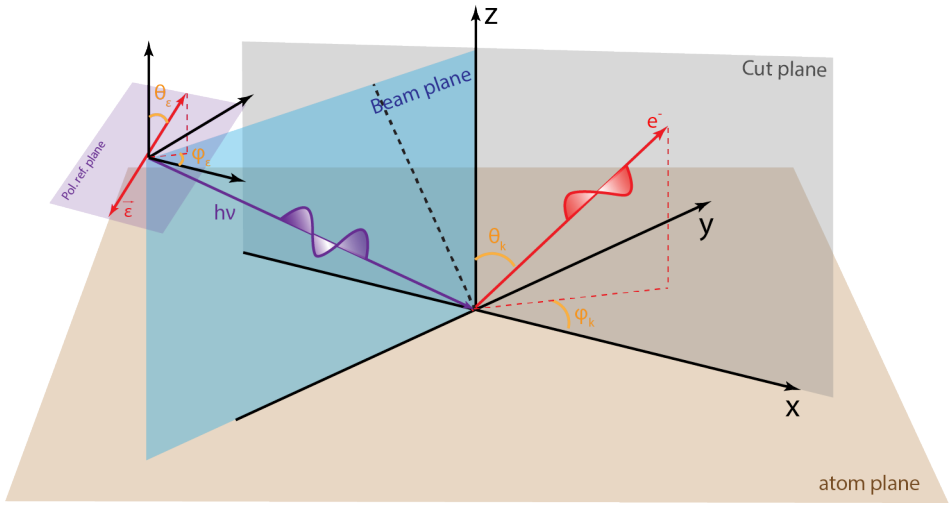

Figure 1: Schematic of coordinate system. The brown, blue, purple, and grey planes are atom plane, beam plane, polarization reference plane, and cut plane, respectively. The direction of electric field of incident photon is defined by $\theta_\varepsilon, \varphi_\varepsilon$ in spherical coordinate system marked in figure. The direction of photoemitted electron is similarly defined by $\theta_{\boldsymbol{k}}, \varphi_{\boldsymbol{k}}$

, where $\beta_{nl}(E_{\text{kin}})$) is termed the asymmetry parameter, and $P_2(\cos\alpha) = \frac{1}{2}(3\cos^2\alpha - 1)$.

If a polarized radiation source is used, then

$$\frac{d\sigma_{nl}}{d\Omega} = \frac{\sigma_{nl}(E_{\text{kin}})}{4\pi}[1 - \frac{1}{2}\beta_{nl}(E_{\text{kin}}))P_2(\cos\gamma)] \tag{1.3.3}$$

, where γ is the angle between the polarization vector and photoelectron direction. The asymmetry parameter takes the form

$$\begin{aligned}\beta_{nl}(E_{\text{kin}}) = \{&l(l-1)R^2_{l-1}(E_{\text{kin}}) + (l+1)(l+2)R^2_{l+1}(E_{\text{kin}}) \\ -6&l(l+1)R_{l-1}(E_{\text{kin}})R_{l+1}(E_{\text{kin}})\cos[\delta_{l+1}(E_{\text{kin}}) - \delta_{l-1}(E_{\text{kin}})]\}/ \\ &\{(2l+1)[lR^2_{l-1}(E_{\text{kin}}) + (l+1)R^2_{l+1}(E_{\text{kin}})]\}\end{aligned} \tag{1.3.4}$$

2 Photo-emission matrix element

As explained above, the matrix element term $\langle\Phi_{E_{\text{kin}},\boldsymbol{k}}|\,\hat{\boldsymbol{\varepsilon}}\cdot\boldsymbol{r}\,|\Phi_{nlx}\rangle$ serves as a dominantly contributing term to the overall photo-emission cross-section. In the following, we will show that the matrix element term depends heavily on the approximations we adopt for the initial state $|\Phi_{nlx}\rangle$ and final state $|\Phi_{E_{\text{kin}},\boldsymbol{k}}\rangle$. To illustrate, we consider the following combinations of approximations:

- scenario 1: bound state under Hartree-Fock central potential as initial state and scatter state under Hartree-Fock central potential as final state;
- scenario 2: hydrogen-like wave function as initial state and free-electron state as final state;

- scenario 3: bound state under Hartree-Fock central potential as initial state and free-electron state as final state;
- scenario 4: hydrogen-like wave function as initial state and scatter state under Hartree-Fock central potential as final state.

2.1 Scenario 1

2.1.1 Initial state

The wave function of initial state can generally be decomposed as a product of radial part and angular part,

$$\langle \boldsymbol{r}|\Phi_{nlx}\rangle = R_{n,l}(r)\sum_{m=-l}^{l} n(m)Y_{l,m}(\theta,\phi) := \frac{P_{n,l}(r)}{r}\sum_{m=-l}^{l} n(m)Y_{l,m}(\theta,\phi) \tag{2.1.1}$$

, where $R_{n,l}(r)$ is the radial part of the wave function with normalization condition:

$$\int_0^\infty P_{n,l}^2(r)dr = 1$$

, $P_{n,l}(r) := rR_{n,l}(r)$, $Y_{l,m}(\theta,\phi)$ is the complex spherical harmonics. By convention, the initial atomic orbital states are indexed by s, p_x, p_y, p_z, d_{xy}, d_{xz}, d_{yz}, $d_{x^2-y^2}$, d_{z^2}, etc., which directly corresponds to real spherical harmonics. The $n(m)$ is the coefficient which transform real spherical harmonics $Y_{l,m}^{(R)}(\theta,\phi)$ into the complex spherical harmonics $Y_{l,m}(\theta,\phi)$ basis by the relation:

$$Y_{l,m}^{(R)} = \begin{cases} \frac{i}{\sqrt{2}}(Y_{l,m} - (-1)^m Y_{l,-m}), & \text{if } m < 0 \\ Y_{l,0}, \quad \text{if } m = 0 \\ \frac{1}{\sqrt{2}}(Y_{l,-m} + (-1)^m Y_{l,m}), & \text{if } m > 0 \end{cases} \tag{2.1.2}$$

The radial part of wave function $P_{n,l}(r) := \frac{R_{n,l}(r)}{r}$ are obtained by solving the one-electron Schrodinger equation

$$[\frac{d^2}{dr^2} + V(r) + \epsilon_{n,l} - \frac{l(l+1)}{r^2}]P_{n,l}(r) = 0 \tag{2.1.3}$$

, where $V(r)$ is the effective central-field potential, and $\epsilon_{n,l}$ is the binding energy. Here, we take the form

$$V(r) = V^H(r) + V^{\text{ex.}}(r) \tag{2.1.4}$$

, where $V^H(r)$ is the standard Hartree potential and $V^{\text{ex.}}(r)$ is the free-electron exchange potential in the Slater form:

$$V^{\text{ex.}}(r) = -6[(\frac{3}{8\pi})\cdot\rho(r)]^{1/3} \tag{2.1.5}$$

, where $\rho(r)$ is the charge density. The asymptotic behavior of $V(r)$ satisfies:

$$\lim_{r\to 0} V(r) = \frac{2Z}{r}; \quad \lim_{r\to\infty} V(r) = \frac{2}{r}$$

, where Z is the nuclear charge.

2.1.2 Final state

We take the final state as the continuum state of one-electron wave function under the same potential in eq. 2.1.4. The final state can be written as a partial-wave expansion

$$\langle \boldsymbol{r}|\Phi_{E_{\text{kin}},\boldsymbol{k}}\rangle = 4\pi \sum_{l',m'} (i)^{l'} \exp(-i\delta_{l'}) Y^*_{l',m'}(\theta_k,\phi_k) Y_{l',m'}(\theta,\phi) R_{E_{\text{kin}},l'}(r) \tag{2.1.6}$$

, where θ_k, ϕ_k is the direction of the photoemited electron in spherical coordinate system (see Figure 1 for schematic drawing) and $Y^*_{l,m}$ is the complex conjugate of Y_{lm} with relation $Y^*_{l,m} = (-1)^m Y_{l,-m}$. $R_{E_{\text{kin}},l'}(r)$ (equivalently, $P_{E_{\text{kin}},l'}/r$) is the radial part of one-electron wave function under effective central potential obtained by solving one-electron Schrodinger equation:

$$[\frac{d^2}{dr^2} + V(r) + E_{\text{kin}} - \frac{l(l+1)}{r^2}] P_{E_{\text{kin}},l}(r) = 0 \tag{2.1.7}$$

, with $E_{\text{kin}} = h\nu - \epsilon_{nl}$. $P_{E_{\text{kin}},l}(r)$ can be normalized by the asymptotic behavior at infinity:

$$\lim_{r\to\infty} P_{\epsilon,l}(r) = \pi^{-1/2}\epsilon^{-1/4} \sin[\epsilon^{1/2} - \frac{1}{2}l\pi - \epsilon^{-1/2}\log(2\epsilon^{1/2}r) + \delta_l(\epsilon)] \tag{2.1.8}$$

, where $\delta_l(\epsilon)$ is the phase shift.

2.1.3 Dipole operator

We express the $\hat{\boldsymbol{\varepsilon}} \cdot \boldsymbol{r}$ in spherical coordinate system by

$$\begin{cases} \varepsilon_x = \sin\theta_\varepsilon \cos\phi_\varepsilon \\ \varepsilon_y = \sin\theta_\varepsilon \sin\phi_\varepsilon \\ \varepsilon_z = \cos\theta_\varepsilon \end{cases} \tag{2.1.9}$$

, where θ_ϵ and ϕ_ϵ are defined in fig. 1 and

$$\begin{cases} x/r = \sin\theta\cos\phi = (2\pi/3)^{1/2}(-Y_{1,1} + Y_{1,-1}) \\ y/r = \sin\theta\sin\phi = i(2\pi/3)^{1/2}(Y_{1,1} + Y_{1,-1}) \\ z/r = \cos\theta = (4\pi/3)^{1/2} Y_{1,0} \end{cases} \tag{2.1.10}$$

2.1.4 Overall expression

Combining eq. 2.1.1, 2.1.6, 2.1.9, 2.1.10, we have

$$\begin{aligned} \langle \Phi_{E_{\text{kin}},\boldsymbol{k}}| \hat{\boldsymbol{\varepsilon}} \cdot \boldsymbol{r} |\Phi_{nlx}\rangle = 4(2/3)^{1/2}\pi^{3/2} \sum_{l',m',m} n(m)(-i)^{l'} \exp(i\delta_{l'}) Y_{l',m'}(\theta_k,\phi_k) R_{n,l'}(E_{\text{kin}}) \\ \times[\varepsilon_x(-\langle l',m'|\,1,1\,|l,m\rangle + \langle l'm'|\,1,-1\,|l,m\rangle) + i\varepsilon_y(\langle l',m'|\,1,1\,|l,m\rangle + \langle l',m'|\,1,-1\,|l,m\rangle) \\ +\sqrt{2}\varepsilon_z \langle l',m'|\,1,0\,|l,m\rangle] \end{aligned} \tag{2.1.11}$$

, where

$$R_{n,l\pm1}(\epsilon) = \int_0^\infty P_{n,l}(r) r P_{\epsilon,l\pm1}(r) dr \tag{2.1.12}$$

and we introduce the notation

$$\begin{aligned}\langle l,m|\,\hat{l},\hat{m}\,|l',m'\rangle &:= \int Y^*_{l,m}(\theta,\phi) Y_{\hat{l},\hat{m}}(\theta,\phi) Y_{l',m'}(\theta,\phi) d\Omega \\ &= \int (-1)^m Y_{l,-m}(\theta,\phi) Y_{\hat{l},\hat{m}}(\theta,\phi) Y_{l',m'}(\theta,\phi) d\Omega \\ =: (-1)^m \sqrt{\frac{3(2l+1)(2l_f+1)}{4\pi}} &\begin{pmatrix} l & \hat{l} & l' \\ 0 & 0 & 0 \end{pmatrix} \begin{pmatrix} l & \hat{l} & l' \\ -m & \hat{m} & m' \end{pmatrix}\end{aligned}$$

. , where in the last line we use the definition of Wigner 3-jm symbols. Specifically, for $\hat{l}=1$, $\langle l,m|\,1,\hat{m}\,|l',m'\rangle$ is only non-zero when

$$\begin{cases} l \pm 1 = l' \\ m + \hat{m} + m' = 0 \end{cases} \tag{2.1.13}$$

, which recovers the dipole selection rule. Eq. 2.1.11 can therefore be simplified as

$$\begin{aligned}\langle \Phi_{E_{\text{kin}},\boldsymbol{k}}|\,\hat{\boldsymbol{\varepsilon}}\cdot\boldsymbol{r}\,|\Phi_{nlx}\rangle = 4(\frac{2}{3})^{1/2}\pi^{3/2} \sum_{l',m} n(m)(-i)^{l'} \exp(i\delta_{l'}) R_{l'}(E_{\text{kin}}) \\ \{\varepsilon_x[-Y_{l',m+1}(\theta_k,\phi_k)\,\langle l',m'|\,1,1\,|l,m\rangle] \\ +i\varepsilon_y[Y_{l',m+1}(\theta_k,\phi_k)\,\langle l',m+1|\,1,1\,|l,m\rangle + Y_{l',m-1}(\theta_k,\phi_k)\,\langle l,m-1|\,1,-1\,|l,m\rangle] \\ +\sqrt{2}\varepsilon_z Y_{l',m}(\theta_k,\phi_k)\,\langle l',m|\,1,0\,|l,m\rangle\}\end{aligned} \tag{2.1.14}$$

Since the summand in eq. 2.1.14 is only non-zero when $l' = l \pm 1$, we can further simplify equation by grouping contributions from $l' = l \pm 1$ into terms $M_{l'=l\pm1}$ and write eq. 2.1.14 as:

$$\langle \Phi_{E_{\text{kin}},\boldsymbol{k}}|\,\hat{\boldsymbol{\varepsilon}}\cdot\boldsymbol{r}\,|\Phi_{nlx}\rangle = (-i)^{l-1}\{\exp(i\delta_{l-1})M_{l-1,x} + \exp(i\delta_{l+1})M_{l+1,x}\} \tag{2.1.15}$$

, where $M_{l'=l\pm1,x}$ is always real and $\delta_{l\pm1}$ is the phase shift. Therefore, the overall matrix element is

$$|\,\langle \Phi_{E_{\text{kin}},\boldsymbol{k}}|\,\hat{\boldsymbol{\varepsilon}}\cdot\boldsymbol{r}\,|\Phi_{nlx}\rangle\,|^2 = M^2_{l+1,x} + M^2_{l-1,x} + 2M_{l+1,x}M_{l-1,x}\cos(\delta_{l+1}-\delta_{l-1}) \tag{2.1.16}$$

, where the last term represents the interference between two photo-emission channels.

For s-orbital, the only contribution comes from $l'=1$ and we therefore have

$$\langle \Phi_{E_{\text{kin}},\boldsymbol{k}}|\,\hat{\boldsymbol{\varepsilon}}\cdot\boldsymbol{r}\,|\Phi_{nlx}\rangle = \sqrt{4\pi}(-i)\exp(i\delta_l)R_1(E_{\text{kin}})(\hat{\boldsymbol{\epsilon}}\cdot\hat{\boldsymbol{k}})$$

For p- and d-orbitals, it is convenient to explicitly tabulate the corresponding $M_{l\pm1}$ below.

p-orbitals:

- p_x:

$$\begin{cases} M_{0,p_x} = 2\sqrt{\pi}R_0[\sqrt{1/3}\varepsilon_x] \\ M_{2,p_x} = 2\sqrt{\pi}R_2[-\sqrt{3/4}\sin^2\theta_k(\varepsilon_x\cos 2\phi_k + \varepsilon_y \sin 2\phi_k) \\ \qquad +\varepsilon_x\sqrt{1/12}(3\cos^2\theta_k - 1) - \varepsilon_z\sqrt{3}\sin\theta_k\cos\theta_k\cos\phi_k] \end{cases}$$

- p_y:

$$\begin{cases} M_{0,p_y} = 2\sqrt{\pi}R_0[\sqrt{1/3}\varepsilon_y] \\ M_{2,p_y} = 2\sqrt{\pi}R_2[\sqrt{3/4}\sin^2\theta_k(-\varepsilon_x\sin 2\phi_k + \varepsilon_y \cos 2\phi_k) \\ \qquad +\varepsilon_y\sqrt{1/12}(3\cos^2\theta_k - 1) - \varepsilon_z\sqrt{3}\sin\theta_k\cos\theta_k\sin\phi_k] \end{cases}$$

- p_z:

$$\begin{cases} M_{0,p_z} = 2\sqrt{\pi}R_0[\sqrt{1/6}\varepsilon_z] \\ M_{2,p_z} = 2\sqrt{2\pi}R_2[\sqrt{3/2}\sin\theta_k\cos\theta_k(-\varepsilon_x\cos\phi_k - \varepsilon_y \sin\phi_k) \\ \qquad -\varepsilon_z\sqrt{1/6}(3\cos^2\theta_k - 1)] \end{cases}$$

d-orbitals:

- $d_{x^2-y^2}$:

$$\begin{cases} M_{1,d_{x^2-y^2}} = -2\sqrt{\pi}R_1[\sqrt{3/5}\sin\theta_k(-\varepsilon_x\cos\phi_k + \varepsilon_y \sin\phi_k)] \\ M_{3,d_{x^2-y^2}} = -2\sqrt{\pi}R_3[\sqrt{3/80}\sin\theta_k(5\cos^2\theta_k - 1)(-\varepsilon_x\cos\phi_k + \varepsilon_y \sin\phi_k) \\ \qquad +\sqrt{15/16}\sin^3\theta_k(\varepsilon_k\cos 3\phi_k + \varepsilon_y \sin 3\phi_k) + \varepsilon_z\sqrt{15/4}\sin^2\theta_k\cos\theta_k\cos 2\phi_k] \end{cases}$$

- d_{z^2}:

$$\begin{cases} M_{1,d_{z^2}} = -2\sqrt{\pi}R_1[\sqrt{1/10}\sin\theta_k(\varepsilon_x\cos\phi_k + \varepsilon_y \sin\phi_k)] \\ M_{3,d_{z^2}} = -2\sqrt{2\pi}R_3[\sqrt{9/40}\sin\theta_k(5\cos^2\theta_k - 1)(\varepsilon_x\cos\phi_k + \varepsilon_y \sin\phi_k) \\ \qquad +\varepsilon_z\sqrt{9/40}(5\cos^3\theta_k - 3\cos\theta_k)] \end{cases}$$

- d_{xz}:

$$\begin{cases} M_{1,d_{xz}} = 2\sqrt{\pi}R_1[\sqrt{3/5}(\varepsilon_x\cos\theta_k + \varepsilon_z \sin\theta_k\cos\phi_k)] \\ M_{3,d_{xz}} = -2\sqrt{\pi}R_3[\sqrt{15/4}\sin^2\theta_k\cos\theta_k(\varepsilon_x\cos 2\phi_k + \varepsilon_y \sin 2\phi_k) \\ \qquad -\varepsilon_x\sqrt{3/20}(5\cos^3\theta_k - 3\cos\theta_k) + \varepsilon_z\sqrt{3/5}\sin\theta_k(5\cos^2\theta_k - 1)\cos\phi_k] \end{cases}$$

- d_{yz}:

$$\begin{cases} M_{1,d_{xz}} = 2\sqrt{\pi}R_1[\sqrt{3/5}(\varepsilon_y\cos(\theta_k) + \varepsilon_z \sin\theta_k\sin\phi_k)] \\ M_{3,d_{xz}} = -2\sqrt{\pi}R_3[\sqrt{15/4}\sin^2\theta_k\cos\theta_k(\varepsilon_x\sin 2\phi_k - \varepsilon_y \cos 2\phi_k) \\ \qquad -\varepsilon_y\sqrt{3/20}(5\cos^3\theta_k - 3\cos\theta_k) + \varepsilon_z\sqrt{3/5}\sin\theta_k(5\cos^2\theta_k - 1)\sin\phi_k] \end{cases}$$

- d_{xy}:

$$\begin{cases} M_{1,d_{yz}} = 2\sqrt{\pi}R_1[\sqrt{3/5}\sin\theta_k(\varepsilon_x\sin\phi_k + \varepsilon_y \cos\phi_k)] \\ M_{3,d_{yz}} = -2\sqrt{2\pi}R_3[\sqrt{3/80}\sin\theta_k(5\cos^2\theta_k - 1)(\varepsilon_x\sin\phi_k + \varepsilon_y \cos\phi_k) \\ \qquad +\sqrt{15/16}\sin^3\theta_k(\varepsilon_x\sin 3\phi_k - \varepsilon_y \cos 3\phi_k) + \varepsilon_z\sqrt{15/4}\sin^2\theta_k\cos\theta_k\sin 2\phi_k] \end{cases}$$

2.2 Scenario 2

2.2.1 Initial state

For the initial state in eq. 2.1.1,

$$\langle \boldsymbol{r}|\Phi_{nlx}\rangle = R_{n,l}(r)\sum_{m=-l}^{l} n(m)Y_{l,m}(\theta,\phi)$$

, we use the hydrogen-like wave function, i.e.

$$R_{n,l}(r) = \sqrt{(\frac{2}{nr_B})^3\frac{(n-l-1)!}{2n(n+l)!}}(\frac{2Zr}{nr_B})^l e^{-\frac{Zr}{nr_B}}L_{n-l-1}^{2l+1}(\frac{2Zr}{nr_B}) \tag{2.2.1}$$

, where r_B is the Bohr radius, Z is the effective nuclear charge (it can be empirically determined by Slater's rules), and $L_{n-l-1}^{2l+1}(\cdot)$ is the generalized Laguerre polynomial.

2.2.2 Final state

We use the free-electron final state and express in the basis of spherical harmonics

$$\langle \boldsymbol{r}|\,|f\rangle = e^{i\boldsymbol{k_f}\cdot\boldsymbol{r}} = 4\pi\sum_{l'=0}^{\infty} j_{l'}(\boldsymbol{k_f}\cdot\boldsymbol{r})\sum_{m'=-l'}^{l'} Y_{l',m'}^*(\theta_k,\phi_k)Y_{l',m'}(\theta,\phi) \tag{2.2.2}$$

, where $j_{l'}(\cdot)$ is the Bessel function, k_f is the wave vector of the electron, and $Y_{l,m}^*(\theta,\phi)$ is the complex conjugate of $Y_{l,m}(\theta,\phi)$.

2.2.3 Overall expression

Combining eq. 2.2.1, 2.1.9, 2.1.10, 2.2.2, we have,

$$\begin{aligned}\langle \Phi_{E_{\text{kin}},\boldsymbol{k}}|\,\hat{\boldsymbol{\varepsilon}}\cdot\boldsymbol{r}\,|\Phi_{nlx}\rangle = 4\sqrt{\frac{2}{3}}\pi^{3/2}\sum_{l'm'm} n(m)(-i)^{l'}(\int j_{l'}(k_f r)R_{n,l}(r)r^3dr)Y_{l',m'}(\theta_k,\phi_k)\\ \{\epsilon_x[\langle l',m'|\,1,1\,|l,m\rangle + \langle l',m'|\,1,-1\,|l,m\rangle]\\ +i\epsilon_y[\langle l',m'|\,1,1\,|l,m\rangle + \langle l',m'|\,1,-1\,|l,m\rangle]\\ +\sqrt{2}\epsilon_z\,\langle l',m'|\,1,0\,|l,m\rangle\}\end{aligned} \tag{2.2.3}$$

Comparing with eq. 2.1.14, the only two difference lie in both the radial integral part and the vanishing phase shift term of final state. Therefore, we can similarly group the contributions from $l' = l \pm 1$ into two terms,

$$\langle \Phi_{E_{\text{kin}},\boldsymbol{k}}|\,\hat{\boldsymbol{\varepsilon}}\cdot\boldsymbol{r}\,|\Phi_{nlx}\rangle = (-i)^{l-1}(X_{l-1,x}+X_{l+1,x}) \tag{2.2.4}$$

and

$$|\,\langle \Phi_{E_{\text{kin}},\boldsymbol{k}}|\,\hat{\boldsymbol{\varepsilon}}\cdot\boldsymbol{r}\,|\Phi_{nlx}\rangle\,|^2 = (X_{l-1,x}+X_{l+1,x})^2 \tag{2.2.5}$$

, with the tabulated expressions in scenario 1 hold under substitution

$$R_{n,l\pm1}(E_{\text{kin}}) \to \int_0^{\infty} j_{l\pm1}(k_f r)R_{n,l}(r)r^3dr \tag{2.2.6}$$

2.3 Scenario 3

In scenario 3, we choose the bound state under Hartree-Fock central potential defined by eq. 2.1.1 as the initial state and free-electron final state defined by eq. 2.2.2. Following a similar derivation, the overall expression is similar to eq. 2.2.3 with the only substitution

$$\int_0^\infty j_{l\pm1}(k_f r) R_{n,l}(r) r^3 dr \to \int_0^\infty j_{l\pm1}(k_f r) P_{n,l}(r) r^2 dr \tag{2.3.1}$$

2.4 Scenario 4

In scenario 4, we choose the hydrogen-like wave function as initial state and scatter state under Hartree-Fock central potential as final state. Following a similar derivation, the overall expression is similar to eq. 2.1.14 with the only substitution

$$R_{n,l\pm1}(\epsilon) = \int_0^\infty P_{n,l}(r) r P_{\epsilon,l\pm1}(r) dr \to R_{n,l\pm1}(\epsilon) = \int_0^\infty R_{n,l}(r) r^2 P_{\epsilon,l\pm1}(r) dr \tag{2.4.1}$$

, where $R_{n,l}$ is defined by eq. 2.2.1 and $P_{\epsilon,l\pm1}$ is defined by eq. 2.1.7.

Yingfei Li
yingfeil@stanford.edu

3 Numerical considerations

3.1 Effective central field potential and energy for bound state

Since $V(r)$ in eq. 2.1.4 depends charge density (eq. 2.1.5), the self-consistent eq. 2.1.3 is solved iteratively by Manson-Cooper algorithm, with details *in D.R. Hartree, The calculation of the atomic structures, chapter 5 (John Wiley & Sons, Inc., New York, 1957).* For computational efficiency, we pre-calculate the intermediate results of $V(r)$ and ϵ_{nl} in our package, which are extracted from the textbook of Herman and Skillman.

3.2 Initial state (bound state)

For initial state in scenario 1, integration of eq. 2.1.3 is calculated inward via finite difference method with $\Delta r = 0.001$ (in Bohr radius), with initial conditions at sufficiently large r:

$$P_{n,l}(100r_c) = 0, \qquad \frac{dP_{n,l}}{dr}(100r_c) = 0$$

, where

$$r_c = \arg\min\{r : |V(r) - \frac{2}{r}| < 10^{-2}\}$$

3.3 Final state (continuum state)

For final state (continuum state) in scenario 1, integration of eq. 2.1.7 is calculated outward via finite difference method with $\Delta r = 0.001$ (in Bohr radius). To obtain the asymptotic behavior of the wave function at small r, we asymptotically expand $V(r)$ by

$$V(r) = \frac{2Z}{r} + 2v_0(r; nl) + \mathcal{O}(r^2) \tag{3.3.1}$$

, where $2v_0$ is the first-order correction to limit at $V(r)_{r\to 0} = \frac{2Z}{r}$. Substitute into eq. 2.1.7, we have:

- $l = 0$:

$$P_{\epsilon,l}(r) = Ar\{1 - Zr + \frac{1}{6}[2N^2 - (2v_0(r; nl) - \epsilon)]r^2 - \frac{1}{18}Z[Z^2 - 2(2v_0(r; nl) - \epsilon]r^3 + \mathcal{O}(r^4)\}$$

- $l = 1$:

$$P_{\epsilon,l}(r) = Ar^2\{1 - \frac{1}{2}Zr + \frac{1}{10}[N^2 - (2v_0(r; nl) - \epsilon)]r^2 - \frac{1}{180}Z[2Z^2 - 7(2v_0(r; nl) - \epsilon]r^3 + \mathcal{O}(r^4)\}$$

- $l = 2$:

$$P_{\epsilon,l}(r) = Ar^3\{1 - \frac{1}{3}Zr + \frac{1}{42}[2Z^2 - 3(2v_0(r; nl) - \epsilon)]r^2 - \frac{1}{252}Z[Z^2 - 5(2v_0(r; nl) - \epsilon)]r^3 + \mathcal{O}(r^4)\}$$

- $l = 3$:

$$P_{\epsilon,l}(r) = Ar^4\{1 - \frac{1}{4}Zr + \frac{1}{36}[Z^2 - 2(2v_0(r; nl) - \epsilon)]r^2 - \frac{1}{1080}Z[2Z^2 - 13(2v_0(r; nl) - \epsilon]r^3 + \mathcal{O}(r^4)\}$$

, where A is the normalization constant. Therefore, the initial condition for outward integration at small r is:

- $l = 0$:
$$P_{\epsilon,l}(r) = Ar; \quad \frac{dP_{\epsilon,l}}{dr}(r) = A$$
- $l = 1$:
$$P_{\epsilon,l}(r) = Ar^2; \quad \frac{dP_{\epsilon,l}}{dr}(r) = 2Ar$$
- $l = 2$:
$$P_{\epsilon,l}(r) = Ar^3; \quad \frac{dP_{\epsilon,l}}{dr}(r) = 3Ar^2$$
- $l = 3$:
$$P_{\epsilon,l}(r) = Ar^4; \quad \frac{dP_{\epsilon,l}}{dr}(r) = 4Ar^3$$

The phase shift $\delta_l(\epsilon)$ of final state is calculated by least-square fit to the radial wave function at sufficiently large r:

$$\delta_l(\epsilon) = \arg\min_{\delta\in[0,2\pi)} \int_{90r_c}^{100r_c} \{\pi^{-1/2}\epsilon^{-1/4}\sin[\epsilon^{1/2} - \frac{1}{2}l\pi - \epsilon^{-1/2}\log(2\epsilon^{1/2}r) + \delta] - P_{\epsilon,l}(r)\}^2 dr \quad (3.3.2)$$

3.4 Conversion from momentum to photo-emission angle

The map from $(h\nu, k_x, k_y)$ to (k_x, k_y, k_z) are given by

$$\begin{aligned} k &= \frac{1}{\hbar}\sqrt{2m_e(h\nu - \epsilon_{nl})} = 0.512\sqrt{h\nu - \epsilon_{nl}} \\ \theta_k &= \arctan(\frac{\sqrt{k_x^2 + k_y^2}}{\sqrt{k^2 - k_x^2 - k_y^2}}) \\ \phi_k &= \begin{cases} \arctan(\frac{k_y}{k_x}), k_y \geq 0 \\ \pi + \arctan(\frac{k_y}{k_x}), k_y < 0 \end{cases} \end{aligned} \quad (3.4.1)$$

, where momentum is in the unit of $1/\mathring{A}$, $\hbar\nu$ in the units of eV.

3.5 Polarization at SSRL BL5-2

At SSRL BL 5-2, for LH (p-) polarization, $\theta_\epsilon = \frac{2\pi}{9}$ and $\phi_\epsilon = \frac{\pi}{2}$. For LV ($s$-) polarization, $\theta_\epsilon = \frac{\pi}{2}$ and $\phi_\epsilon = 0$.

4 Package install

The package is written under Python 3.8 and utilizes parallel computation. The source codes and examples are available at https://github.com/Infi-Yingfei-Li/arpes_simulation.